The decadal variation in displacement sudden stratospheric warmings driven by Pacific teleconnections

Yuanpu Li[1] and Zhiping Wen[1]

[1]Institute of Atmospheric Sciences, Fudan University

November 23, 2022

Abstract

Sudden stratospheric warmings (SSWs) are important processes that exert impacts on tropospheric weather and climate. This study used the duration to describe the variations in the displacement SSWs and defined Pacific–North American (PNA) and Western Pacific (WP) combined indices (PWC Index) to describe the combinations of PNA and WP. We found that the duration of the displacement SSWs (SSW1) first increased and then decreased around 2000. The decadal variation in SSW1 can be explained by PWC Index, since the teleconnection combinations with the same signs (+PNA+WP/-PNA-WP) can affect upward planetary wave 1 and SSW1 more efficiently than +PNA-WP/-PNA+WP. The second mode of tropical Pacific sea surface temperature plays a more important role in modulating the decadal variations in PWC Index and displacement SSWs than the first mode.

Hosted file

gyuanpuli_grl_resubmit_final.docx available at https://authorea.com/users/543321/articles/601236-the-decadal-variation-in-displacement-sudden-stratospheric-warmings-driven-by-pacific-teleconnections

The decadal variation in displacement sudden stratospheric warmings driven by Pacific teleconnections

Yuanpu Li[1*] and Zhiping Wen[1*]

1 Institute of Atmospheric Sciences, Fudan University, Shanghai, China

*Corresponding author:

Yuanpu Li (liyuanpu@fudan.edu.cn)

ORCID: https://orcid.org/0000-0003-3047-5675

Zhiping Wen (zpwen@fudan.edu.cn)

ORCID: https://orcid.org/0000-0003-0178-9835

Key Points:

Main point #1:

A new index describing the combined impact of PNA and WP is defined to explain the decadal variation in SSWs.

Main point #2:

+PNA+WP and -PNA-WP have an essential role in modulating planetary wave 1 and displacement SSWs.

Main point #3:

The second mode of tropical Pacific SST modulates the decadal variation in PWC Index and displacement SSWs.

Abstract

Sudden stratospheric warmings (SSWs) are important processes that exert impacts on tropospheric weather and climate. This study used the duration to describe the variations in the displacement SSWs and defined Pacific–North American (PNA) and Western Pacific (WP) combined indices (PWC Index) to describe the combinations of PNA and WP. We found that the duration of the displacement SSWs (SSW1) first increased and then decreased around 2000. The decadal variation in SSW1 can be explained by PWC Index, since the teleconnection combinations with the same signs (+PNA+WP/−PNA−WP) can affect upward planetary wave 1 and SSW1 more efficiently than +PNA−WP/−PNA+WP. The second mode of tropical Pacific sea surface temperature plays a more important role in modulating the decadal variations in PWC Index and displacement SSWs than the first mode.

Plain Language Summary

The low-frequency variation in SSWs can effectively modulate the tropospheric climate change, which highlights the importance of studying the decadal variation in SSWs. However, it is unclear if the low-frequency variations in SSWs occur by chance or due to external factors. Both individual Pacific-North America (PNA) and Western Pacific (WP) teleconnection can affect SSWs, but there is no index to describe the combined impact of PNA and WP on SSWs. This study used the coordinate rotation method to define PNA and WP combined indices (PWC Index). We found that the decadal variation in the duration of displacement SSWs is consistent with that in the combinations of PNA and WP. The second principal component of the Pacific sea surface temperature also plays essential roles in modulating the decadal variations in the teleconnections and SSWs. The potential application of PWC Index may be extended to on other tropospheric climate change.

Keywords: teleconnection; sudden stratospheric warmings; decadal variation

Introduction

Sudden stratospheric warmings (SSWs) are rapid temperature-rising processes that occur in the polar stratosphere in winter. During SSW, the mid-to-upper stratosphere in the polar region rises by more than 40 K in a few days (*Butler et al.*, 2015). Weak polar vortex events or SSWs are related to the negative North Atlantic Oscillation or Arctic Oscillation anomalies and southward shift of storm tracks in Europe (*Baldwin and Dunkerton*, 2001; *Baldwin et al.*, 2021; *Polvani et al.*, 2017). Just as many strong warmings had an important effect on the troposphere, some minor warmings (*Domeisen and Butler*, 2020; *Hendon et al.*, 2019; *Lim et al.*, 2019; *Rao et al.*, 2020; *Wang and Chen*, 2010) were related to the tropospheric weather anomalies. SSWs in this study include both major and minor SSWs. SSWs can be classified into two types: vortex-displacement and vortex-splitting (*Charlton and Polvani*, 2007). These types of SSWs have different impacts on the troposphere (*White et al.*, 2021). The vortex-displacement SSWs are mostly preceded by planetary wave 1 (PW1) anomalies, while vortex-splitting SSWs are preceded by either PW1 or planetary wave 2 (PW2) anomalies (*Ayarzagüena et al.*, 2019; *Bancalá et al.*, 2012; *Barriopedro and Calvo*, 2014; *Smith and Kushner*, 2012). The SSWs preceded by PW1 forcing are abbreviated as SSW1, and the SSWs preceded by PW2 anomalies are abbreviated as SSW2. The low-frequency variation in SSWs can effectively modulate the Atlantic Meridional Overturning Circulation (*Reichler et al.*, 2012), which highlights the importance of studying the decadal-scale variation in SSWs. However, it is unclear if the decadal-scale variability of SSWs occurred by chance or partially due to external factors such as oceanic variability (*Baldwin et al.*, 2021).

The Pacific–North American (PNA) teleconnection and Western Pacific (WP) teleconnection are the two dominant tropospheric modes in the Pacific winter (*Linkin and Nigam*, 2008). Both teleconnections effectively interfere with the low height center over the subpolar North Pacific, which is a key region to trigger SSWs (*Garfinkel et al.*, 2010; *Garfinkel et al.*, 2012). Therefore, the PNA and WP teleconnections are good precursors of SSWs and they can jointly affect SSWs (*Bao et al.*, 2017; *Dai and Tan*, 2016). Previous studies have found that though PNA and WP are the atmospheric internal dynamic variabilities, they are modulated by tropical and extratropical Pacific SST (*e.g., Dai and Tan,* 2019*; Hu and Guan,* 2018; *Hu et al.,* 2021; *Hurwitz et al.,* 2012; *Li et al.,* 2019; *Liu et al.,* 2020; *Straus and Shukla,* 2000; 2002).

The forcing associated with the Pacific sea surface temperature (SST) plays an important role in modulating SSWs. El Niño-Southern Oscillation (ENSO) is the leading mode of SST in the tropical Pacific (*Feng et al.*, 2020). El Niño-related tropical forcing induces more upward Rossby wave propagation into the stratosphere and a weakened vortex, while La Niña induces a general opposite process to El Niño (*Barriopedro and Calvo*, 2014; *Garfinkel and Hartmann*, 2008; *Li and Lau*, 2013). However, over the past 40 years, there have been more SSWs in La Niña than El Niño (*Domeisen et al.*, 2019). There is less consensus regarding whether Modoki El Niño weakens the stratospheric polar vortex (*Calvo et al.*, 2017; *Domeisen et al.*, 2019; *Garfinkel et al.*, 2013; *Xie et al.*, 2012). The impact of Modoki La Niña (MLN) on

SSW has received less attention because the response of the Arctic stratosphere to La Niña is relatively weak compared to El Niño (*Xie et al.*, 2018).

This study proposed a new index to describe the combined impact of PNA and WP, which can explain the decadal variation in the displacement SSWs. The origin of the decadal variation in the combinations of PNA and WP is attributed to the second mode of tropical Pacific SST.

Data and Methods

ERA5 (*Hersbach et al.*, 2020) and NCEP (*Kalnay et al.*, 1996), and JRA55 (*Kobayashi et al.*, 2015) reanalysis provided geopotential height, wind, and temperature data. HadISST (*Rayner et al.*, 2003) provided SST data.

Definitions of the climate indices

PNA and WP indices. The PNA and WP are defined by the modified pointwise method, which is proposed by Climate Prediction Center of NOAA. (https://www.cpc.ncep.noaa.gov/products/precip/CWlink/pna/month_pna_index2.shtml; https://psl.noaa.gov/data/timeseries/daily/WPO/).

PWC Index. PNA and WP combined indices (PWC Index) are obtained by rotating the coordinate axes, which is illustrated in Fig. 1a. Since the correlation coefficient between PNA and WP in 1979-2020 is 0.03, the two indices can be considered orthogonal. Any year can be represented as a point in a Cartesian coordinate system with the PNA and WP indices as the black axes. Then rotate the coordinate axes 45° to the right to get the red coordinate axes. The value of any point projected onto the first axis is defined as **PWC1**, and the value projected onto the second axis is defined as **PWC2**. The formula for projection is as follows:

$$PWC1 = \frac{\sqrt{2}}{2}PNA + \frac{\sqrt{2}}{2}WP$$
$$PWC2 = \frac{\sqrt{2}}{2}PNA - \frac{\sqrt{2}}{2}WP$$

The newly obtained indices are continuous scalar (shown in Fig. 1b). A positive PWC1 indicates a feature with +PNA+WP, and a negative PWC1 indicates a feature with -PNA-WP. A positive PWC2 indicates a feature with +PNA-WP, and a negative PWC2 indicates a feature with -PNA+WP.

+PNA+WP/−PNA−WP index. If winter has positive PNA and positive WP index, then the winter is assigned with a value of +1. If winter has negative PNA and negative WP index, then the winter is assigned with a value of -1.

+PNA−WP/−PNA+WP index. If winter has a positive PNA and negative WP index, then the winter is assigned with a value of +1. If winter has a negative PNA and positive WP index, then the winter is assigned with a value of −1.

SSWs. SSWs are defined when the daily temperature gradient between 60°N and 90°N at 10 hPa becomes positive, including both minor and major warmings. Only warmings during December–February are counted.

SSW duration. SSWs were classified into wave-1 and wave-2 events according to the method proposed by *Barriopedro and Calvo* (2014). We defined Z1 and Z2 as the daily amplitudes of PW1 and PW2 in geopotential height at 50 hPa, 60°N obtained by Fourier decomposition.

If a day from December to February satisfies the following criterion, then this day is added to **SSW1 duration**: the gradient of temperature between 60°N and 90°N at 10 hPa at this day becomes positive; Z2−Z1 < 200 m is satisfied for the entire previous 10 days before this day, and [Z2] < [Z1] (the brackets denote the averaged amplitude of Z1 and Z2 of the previous 10 days).

If a day from December to February satisfies the following criterion, then this day is added to **SSW2 duration**: the gradient of temperature between 60°N and 90°N at 10 hPa at this day becomes positive; Z2−Z1 ≥ 200 m persists for more than 1 day within the 10 days before this day, or [Z2] ≥ [Z1]. The total numbers of SSW1 and SSW2 days in the winter (December−February) are the duration of SSW1 and SSW2.

The Eliassen-Palm (EP) flux and its divergence are calculated using the same method introduced by *Andrews et al.* (1987).

SST-PC1 and SST-PC2. The December to February SST fields were detrended, and then EOF analysis is exerted on SST over the domain of 30°S–30°N, 120°E–100°W to distinguish the two main modes.

Statistics

A Monte Carlo test has been adopted to determine the statistical significance of the deviations from climatology during different teleconnection combinations (Fig. 4). We randomly subsampled elements from all winters and averaged the result. The number of sub-samples matches the number of each teleconnection combination. We repeated this random selection process 1,000,000 times to obtain a probability density function. The significance of the deviation was estimated using the density function.

The consistency of SSW1 and PWC1

The duration of SSW1 experienced a decadal-scale variation that reached a peak around 2003 (Fig. 2e), while the duration of SSW2 had no obvious decadal-scale changes since 1979. Past studies documented that the frequency of major SSWs had experienced decadal-scale variation. *Reichler et al.*, (2012) showed the peak of the moving average of major SSWs was reached around 1995. *Butler et al.* (2017) have pointed there were relatively more SSWs in the 2000s than in the 1990s. PWC1 has a similar decadal variation as SSW1, and the correlation coefficient of the moving average of the two climate indices is 0.9 (Table 1). The decadal variation in PWC2 is not consistent with that in SSW1. The correlation between PWC1 and SSW1 is higher than the correlation between single PNA or WP and SSW1, no matter on the interannual or decadal scale. Fig. 2a and 2b show binary indices to describe the combinations of PNA and WP. The results in Fig. 2a and 2b are obtained by dividing the phases of PNA and WP with 0 as the threshold. If other threshold values are used, the decadal variation curve of +PNA+WP/−PNA−WP will not change significantly. The 11-year moving average of +PNA+WP/−PNA−WP is consistent with that of PWC1. The binary indices are convenient to facilitate composite analysis, thus the composite results of Fig. 3 and 4 are based on Fig. 2a and 2b. The consistency among the moving averages of SSW1, PWC1, +PNA+WP/−PNA−WP implies the decadal variation in the displacement SSWs originates from the decadal change in the combined effects of PNA and WP.

The SSW1 also have a higher positive correlation with PWC1 than PWC2, single

PNA or WP index on interannual scale (Table 1). This indicates that the decadal-scale consistency of SSW1 and PWC1 is based on the mechanism of interannual-scale connection between them. Figure 3a shows that the centers of the PW1 component of the height anomalies during +PNA+WP are in-phase with the climatological pattern of PW1. This pattern implies a strengthened PW1 in the upper troposphere and opposite for −PNA−WP. The anomalous centers of +PNA−WP and −PNA+WP are not overlapped with the climatological centers, and their anomalies are smaller than those of +PNA+WP and −PNA−WP. Therefore, the impacts of +PNA−WP and −PNA+WP on the PW1 are smaller than those of +PNA+WP and −PNA−WP. During +PNA+WP pattern, PW1 propagating to the stratosphere has increased significantly, accompanied by the convergence of EP fluxes in the polar stratosphere. During −PNA−WP pattern, PW1 propagating to the stratosphere has reduced significantly, accompanied by the divergence of EP fluxes in the polar stratosphere. +PNA−WP and −PNA+WP have little effect on upward propagating of PW1 (Fig. 3c). The PW2 anomalies of +PNA+WP are in disagreement with climatology PW2, whereas those of −PNA−WP are in agreement with climatology PW2 (Fig. 3b). There are more (less) PW2 EP fluxes propagating to the stratosphere during −PNA−WP (+PNA+WP) (Fig. 3d). This explains why PWC1 is negatively correlated with the duration of SSW2 on an interannual scale.

The SSW1 duration appears longer (shorter) during +PNA+WP (−PNA−WP), corresponding to the significant enhancement (weakening) of PW1 propagated to the stratosphere. The deviations of SSW1 duration of +PNA−WP and −PNA+WP from the climatology are negligible (Fig. 4a). For the duration of SSW2, only +PNA+WP and −PNA+WP statistically significantly deviate from the climatology (Fig. 4b). Yet, the anomalies in SSW2 duration during −PNA+WP are challenging to explain from divergence of PW2. During the analysis of distribution of a major SSW duration, we use ERA5 and NCEP from 1950 to 2020 and JRA55 from 1958 to 2020 since winters without major SSWs appear very frequently during these years and longer data record ensures the robustness of the results. The distribution of major SSW duration in different teleconnection combinations is consistent with the distribution of SSW duration.

The Pacific SST origin of the decadal variation in PWC1

The first two principal components derived from empirical orthogonal function (EOF) analysis on the winter tropical Pacific SST (30°S–30°N) are shown in Fig. 2f. The regressed SST anomalies of the first principal component (SST-PC1) corresponds to Eastern Pacific El Niño (EEN) with a dipole pattern (Fig. 5c), while the regressed SST anomalies of the second principal component (SST-PC2) resemble Modoki La Niña (MLN) with a tripole pattern (Fig. 5d) (*Ashok and Yamagata*, 2009; *Feng et al.*, 2020). The regressed SST anomalies of PWC1 (Fig. 5b) also have a tripole pattern similar to SST-PC2, while the regressed SST anomalies of PWC2 (Fig. 5a) have a dipole pattern similar to SST-PC1. The interannual correlation coefficients show that PWC1 is strongly related to SST-PC2, while PWC2 is more related to SST-PC1. The correlation coefficients of the moving averaged indices show that the decadal variation in SST-PC2 is more consistent with that in PWC1 than in SST-PC1 (also see Fig. 2e).

Previous studies have pointed out that different modes of tropical and extratropical SST anomalies can modulate PNA (*Johnson and Feldstein*, 2010) and WP (*Dai and Tan*, 2016; *Furtado et al.*, 2012; *Liu et al.,* 2020; *Hu et al.,* 2021). There are positive SST anomalies in the eastern and western boundary of the tropical Pacific in the pattern of SST-PC2. The warming from 150°W to 110°W is located over the region where the climatology of the SST is above 25°C and above the threshold for convection to trigger (*Johnson and Xie*, 2010). The warming in this region causes Gill response (*Gill*, 1980), an anticyclone pair propagating Rossby waves northward to the extratropical Pacific. Therefore, the positive SST anomalies in the eastern Pacific favor the occurrence of +PNA (*Horel and Wallace*, 1981; *Li and Wen*, 2021). The warming of tropical eastern Pacific SST can promote the evolution of the synoptic-scale +PNA anomalies into +WP anomalies (*Dai and Tan*, 2016). Moreover, when the western Pacific boundary current tends to be warmer, +WP is more likely to emerge (*Li et al.*, 2018; *Hu et al.,* 2021). *Hurwitz et al.,* (2012) performed two sets of sensitivity experiments using fixed North Pacific (north of 20°N) SST boundary conditions. The pattern of the differences in SST between the two experiment sets (Fig. 1d in *Hurwitz et al.,* 2012) is similar to the regressed SST anomalies to SST-PC2 (north of 20°N) (the signs of anomalies are opposite). Their result implies that the associated extratropical Pacific SST with SST-PC2 contributes to the enhancement of +WP. However, the understanding of the evolution of WP is less comprehensive than that of PNA (*Dai and Tan,* 2019). The relationship between SST and WP needs further research in the future.

Summary and discussion

Based on previous studies, this study used SSW duration to study the decadal variation in the displacement SSWs and proposed a new PWC Index to describe the joint impact of PNA and WP. Although the frequencies of SSWs in some winters are the same, the differences in the duration reflect more information about SSWs, which is helpful to find the factors that affect the interannual and decadal variation in SSWs through correlation analysis. PWC Indices are continuous scalar indices, which include the year-to-year differences in the PNA and WP combinations, bringing convenience to correlation analysis. This study found that PWC1 or +PNA+WP/−PNA−WP could explain the decadal variation in the displacement SSWs.

This study suggested SST-PC2 is the origin of the decadal variation in PWC1, in which both tropical and extratropical SST anomalies related to SST-PC2 could contribute to the change of PNA and WP. SST-PC2 first regulates PWC1, and then, PWC1 affects the SSW1. On the interannual scale, SST-PC2 and SSW1 have a positive correlation, in other words, positive SST-PC2 (corresponding to Modoki La Niña; based on Ashok and Yamagata, 2009) favors the occurrence of SSW1, while negative SST-PC2 (corresponding to Modoki El Niño) is unfavorable for the occurrence of SSW1. *Hegyi and Deng* (2011) and Xie *et al.*, (2019) also stated that

Modoki El Niño leads to a strengthened vortex (fewer SSWs occur). The interannual correlation coefficients show that SST-PC1 has a more significant impact on SSW1 than SST-PC2. However, the decadal variation in SSW1 is more consistent with SST-PC2 rather than SST-PC1. It is still not fully understood to what extent ENSO diversity affects SSWs (*Domeisen et al.*, 2019). Previous studies on Modoki ENSO also have found that it is difficult to objectively define Modoki La Niña separate from canonical La Niña, as there is less inter-event diversity in the SST pattern for La Niña events (Garfinkel et al 2013; Capotondi et al 2015). The stratospheric response is also sensitive to different indices describing Modoki ENSO (Garfinkel et al 2013). Therefore, although we found the relationship between SST-PC2 and SSW1, we are cautious to use the expression that Modoki La Niña favors SSW1.

The PNA and WP teleconnections are the internal variabilities of the atmosphere. There are mutual feedbacks between the tropical ocean and the extratropical atmosphere teleconnection because North Pacific Oscillation or WP variation can also modulate the SST-PC2 through the Pacific meridional mode (Fig. 3 in *Di Lorenzo et al.,* 2015). It is challenging to separate the cause-and-effect relationship of the SST-PC2 and PWC1. Although the decadal changes in Pacific SST and teleconnections are not independent of each other, both of they are the origins of the decadal variations in the displacement SSWs.

Acknowledgments

This work was supported jointly by the National Natural Science Foundation of China

(41805029, 41875087, 42030601) and China Postdoctoral Science Foundation (2018M641913). Thanks to the two anonymous reviewers for their valuable advices.

Open Research

Data Availability Statement

ERA5, NCEP, JRA55 and HadISST are publicly available on the following websites.

ERA5: https://doi.org/10.24381/cds.bd0915c6

NCEP: https://psl.noaa.gov/data/gridded/data.ncep.reanalysis.html

JRA55: https://doi.org/10.5065/D6HH6H41

HadISST: https://www.metoffice.gov.uk/hadobs/hadisst/data/download.html

Competing interests

The Authors declare no Competing Financial or Non-Financial Interests.

References

Andrews, D. G., J. R. Holton, and C. B. Leovy (1987), Middle atmosphere dynamics, Academic press.

Ashok, K., and T. Yamagata (2009), The El Niño with a difference, Nature, 461(7263), 481-484.

Ayarzagüena, B., F. M. Palmeiro, D. Barriopedro, N. Calvo, U. Langematz, and K. Shibata (2019), On the representation of major stratospheric warmings in reanalyses, Atmos.

Chem. Phys., 19(14), 9469-9484.

Baldwin, M. P., and T. J. Dunkerton (2001), Stratospheric Harbingers of Anomalous Weather Regimes, Science, 294(5542), 581-584.

Baldwin, M. P., et al. (2021), Sudden Stratospheric Warmings, Reviews of Geophysics, 59(1), e2020RG000708.

Bancalá, S., K. Krüger, and M. Giorgetta (2012), The preconditioning of major sudden stratospheric warmings, Journal of Geophysical Research: Atmospheres, 117(D4).

Bao, M., X. Tan, D. L. Hartmann, and P. Ceppi (2017), Classifying the tropospheric precursor patterns of sudden stratospheric warmings, Geophysical Research Letters, 44(15), 8011-8016.

Barriopedro, D., and N. Calvo (2014), On the Relationship between ENSO, Stratospheric Sudden Warmings, and Blocking, Journal of Climate, 27(12), 4704-4720.

Butler, A. H., J. P. Sjoberg, D. J. Seidel, and K. H. Rosenlof (2017), A sudden stratospheric warming compendium, Earth Syst. Sci. Data, 9(1), 63-76.

Butler, A. H., D. J. Seidel, S. C. Hardiman, N. Butchart, T. Birner, and A. Match (2015), Defining Sudden Stratospheric Warmings, Bulletin of the American Meteorological Society, 96(11), 1913-1928.

Calvo, N., M. Iza, M. M. Hurwitz, E. Manzini, C. Peña-Ortiz, A. H. Butler, C. Cagnazzo, S. Ineson, and C. I. Garfinkel (2017), Northern Hemisphere Stratospheric Pathway of Different El Niño Flavors in Stratosphere-Resolving CMIP5 Models, Journal of Climate, 30(12), 4351-4371.

Capotondi, A., et al. (2015), Understanding ENSO Diversity, Bulletin of the American

Meteorological Society, 96(6), 921-938.

Charlton, A. J., and L. M. Polvani (2007), A New Look at Stratospheric Sudden Warmings. Part I: Climatology and Modeling Benchmarks, Journal of Climate, 20(3), 449-469.

Dai, Y., and B. Tan (2016), The western Pacific pattern precursor of major stratospheric sudden warmings and the ENSO modulation, Environmental Research Letters, 11(12), 124032.

Dai, Y., and B. Tan (2019), Two Types of the Western Pacific Pattern, Their Climate Impacts, and the ENSO Modulations, Journal of Climate, 32(3), 823-841.

Di Lorenzo, E., G. Liguori, N. Schneider, J. C. Furtado, B. T. Anderson, and M. A. Alexander (2015), ENSO and meridional modes: A null hypothesis for Pacific climate variability, Geophysical Research Letters, 42(21), 9440-9448.

Domeisen, D. I. V., and A. H. Butler (2020), Stratospheric drivers of extreme events at the Earth’s surface, Communications Earth & Environment, 1(1), 59.

Domeisen, D. I. V., C. I. Garfinkel, and A. H. Butler (2019), The Teleconnection of El Niño Southern Oscillation to the Stratosphere, Reviews of Geophysics, 57(1), 5-47.

Feng, Y., X. Chen, and K.-K. Tung (2020), ENSO diversity and the recent appearance of Central Pacific ENSO, Climate Dynamics, 54(1), 413-433.

Furtado, J. C., E. Di Lorenzo, B. T. Anderson, and N. Schneider (2012), Linkages between the North Pacific Oscillation and central tropical Pacific SSTs at low frequencies, Climate Dynamics, 39(12), 2833-2846.

Garfinkel, C. I., and D. L. Hartmann (2008), Different ENSO teleconnections and their effects on the stratospheric polar vortex, Journal of Geophysical Research: Atmospheres, 113(D18).

Garfinkel, C. I., D. L. Hartmann, and F. Sassi (2010), Tropospheric Precursors of Anomalous Northern Hemisphere Stratospheric Polar Vortices, Journal of Climate, 23(12), 3282-3299.

Garfinkel, C. I., M. M. Hurwitz, D. W. Waugh, and A. H. Butler (2013), Are the teleconnections of Central Pacific and Eastern Pacific El Niño distinct in boreal wintertime?, Climate Dynamics, 41(7), 1835-1852.

Garfinkel, C. I., A. H. Butler, D. W. Waugh, M. M. Hurwitz, and L. M. Polvani (2012), Why might stratospheric sudden warmings occur with similar frequency in El Niño and La Niña winters?, Journal of Geophysical Research: Atmospheres, 117(D19).

Gill, A. E. (1980), Some simple solutions for heat-induced tropical circulation, Quarterly Journal of the Royal Meteorological Society, 106(449), 447-462.

Hegyi, B. M., and Y. Deng (2011), A dynamical fingerprint of tropical Pacific sea surface temperatures on the decadal-scale variability of cool-season Arctic precipitation, Journal of Geophysical Research: Atmospheres, 116(D20).

Hendon, H. H., et al. (2019), Rare forecasted climate event under way in the Southern Hemisphere, Nature, 573(7775), 495.

Hersbach, H., et al. (2020), The ERA5 global reanalysis, Quarterly Journal of the Royal Meteorological Society, 146(730), 1999-2049.

Horel, J. D., and J. M. Wallace (1981), Planetary-Scale Atmospheric Phenomena Associated with the Southern Oscillation, Monthly Weather Review, 109(4), 813-829.

Hu, D., and Z. Guan (2018), Decadal Relationship between the Stratospheric Arctic Vortex and Pacific Decadal Oscillation, Journal of Climate, 31(9), 3371-3386.

Hu, D., Z. Guan, M. Liu, and W. Feng (2021), Dynamical mechanisms for the recent ozone depletion in the Arctic stratosphere linked to North Pacific sea surface temperatures, Climate Dynamics.

Hurwitz, M. M., P. A. Newman, and C. I. Garfinkel (2012), On the influence of North Pacific sea surface temperature on the Arctic winter climate, J. Geophys. Res., 117, D19110.

Johnson, N. C., and S.-P. Xie (2010), Changes in the sea surface temperature threshold for tropical convection, Nature Geoscience, 3(12), 842-845.

Johnson, N. C., and S. B. Feldstein (2010), The Continuum of North Pacific Sea Level Pressure Patterns: Intraseasonal, Interannual, and Interdecadal Variability, Journal of Climate, 23(4), 851-867.

Kalnay, E., et al. (1996), The NCEP/NCAR 40-Year Reanalysis Project, Bulletin of the American Meteorological Society, 77(3), 437-472.

Kobayashi, S., et al. (2015), The JRA-55 Reanalysis: General Specifications and Basic Characteristics, Journal of the Meteorological Society of Japan. Ser. II, 93(1), 5-48.

Li, X., Z.-Z. Hu, P. Liang, and J. Zhu (2019), Contrastive Influence of ENSO and PNA on Variability and Predictability of North American Winter Precipitation, Journal of Climate, 32(19), 6271-6284.

Li, Y., and N.-C. Lau (2013), Influences of ENSO on Stratospheric Variability, and the Descent of Stratospheric Perturbations into the Lower Troposphere, Journal of Climate, 26(13), 4725-4748.

Li, Y., and Z. Wen (2021), Influence of tropical convective enhancement in Pacific on the trend of stratospheric sudden warmings in Northern Hemisphere, Climate Dynamics.

Li, Y., W. Tian, F. Xie, Z. Wen, J. Zhang, D. Hu, and Y. Han (2018), The connection between the second leading mode of the winter North Pacific sea surface temperature anomalies and stratospheric sudden warming events, Climate Dynamics, 51(1), 581-595.

Lim, E.-P., H. H. Hendon, G. Boschat, D. Hudson, D. W. J. Thompson, A. J. Dowdy, and J. M. Arblaster (2019), Australian hot and dry extremes induced by weakenings of the stratospheric polar vortex, Nature Geoscience, 12(11), 896-901.

Linkin, M. E., and S. Nigam (2008), The North Pacific Oscillation–West Pacific Teleconnection Pattern: Mature-Phase Structure and Winter Impacts, Journal of Climate, 21(9), 1979-1997.

Liu, M., D. Hu, and F. Zhang (2020), Connections Between Stratospheric Ozone Concentrations Over the Arctic and Sea Surface Temperatures in the North Pacific, Journal of Geophysical Research: Atmospheres, 125(4), e2019JD031690.

Polvani, L. M., L. Sun, A. H. Butler, J. H. Richter, and C. Deser (2017), Distinguishing Stratospheric Sudden Warmings from ENSO as Key Drivers of Wintertime Climate Variability over the North Atlantic and Eurasia, Journal of Climate, 30(6), 1959-1969.

Rao, J., C. I. Garfinkel, I. P. White, and C. Schwartz (2020), The Southern Hemisphere Minor Sudden Stratospheric Warming in September 2019 and its Predictions in S2S Models, Journal of Geophysical Research: Atmospheres, 125(14), e2020JD032723.

Rayner, N. A., D. E. Parker, E. B. Horton, C. K. Folland, L. V. Alexander, D. P. Rowell, E. C. Kent, and A. Kaplan (2003), Global analyses of sea surface temperature, sea ice, and night marine air temperature since the late nineteenth century, Journal of Geophysical

Research: Atmospheres, 108(D14).

Reichler, T., J. Kim, E. Manzini, and J. Kröger (2012), A stratospheric connection to Atlantic climate variability, Nature Geoscience, 5(11), 783-787.

Smith, K. L., and P. J. Kushner (2012), Linear interference and the initiation of extratropical stratosphere-troposphere interactions, Journal of Geophysical Research: Atmospheres, 117(D13).

Straus, D. M., and J. Shukla (2000), Distinguishing between the SST-forced variability and internal variability in mid-latitudes: Analysis of observations and GCM simulations, Quart. J. Roy. Meteor. Soc., 126, 2323-2350.

Straus, D. M., and J. Shukla (2002), Does ENSO force the PNA?, J. Climate, 15, 2340-2358.

Wang, L., and W. Chen (2010), Downward Arctic Oscillation signal associated with moderate weak stratospheric polar vortex and the cold December 2009, Geophysical Research Letters, 37(9).

White, I. P., C. I. Garfinkel, J. Cohen, M. Jucker, and J. Rao (2021), The Impact of Split and Displacement Sudden Stratospheric Warmings on the Troposphere, Journal of Geophysical Research: Atmospheres, 126(8), e2020JD033989.

Xie, F., J. Li, W. Tian, J. Feng, and Y. Huo (2012), Signals of El Niño Modoki in the tropical tropopause layer and stratosphere, Atmos. Chem. Phys., 12(11), 5259-5273.

Xie, F., X. Zhou, J. Li, C. Sun, J. Feng, and X. Ma (2018), The key role of background sea surface temperature over the cold tongue in asymmetric responses of the Arctic stratosphere to El Niño–Southern Oscillation, Environmental Research Letters, 13(11), 114007.

Zhang, J., W. Tian, M. P. Chipperfield, F. Xie, and J. Huang (2016), Persistent shift of the Arctic polar vortex towards the Eurasian continent in recent decades, Nature Climate Change, 6(12), 1094-1099.

Tables

Table 1. The correlation coefficients between different climate indices of interannual (raw time series) and decadal (11-year moving averages) time scale. * one-tailed t-test at the 90% significance level (** for 95%; *** for 99%).

Interannual	SST-PC1	SST-PC2	PWC1	PWC2	PNA	WP
PWC1	0.49***	0.51***	/	/	/	/
PWC2	0.37**	-0.34**	/	/	/	/
SSW1	0.38**	0.28**	0.58***	0.08	0.46***	0.33**
SSW2	-0.29**	-0.06	-0.34**	-0.21	-0.40**	-0.09

11yr	SST-PC1	SST-PC2	PWC1	PWC2	PNA	WP
PWC1	-0.2	0.71***	/	/	/	/
PWC2	0.52***	-0.22*	/	/	/	/
SSW1	-0.29**	0.76***	0.91***	-0.20	0.49***	0.69***
SSW2	-0.39***	-0.19	-0.52***	-0.23*	-0.55***	-0.16

Figures

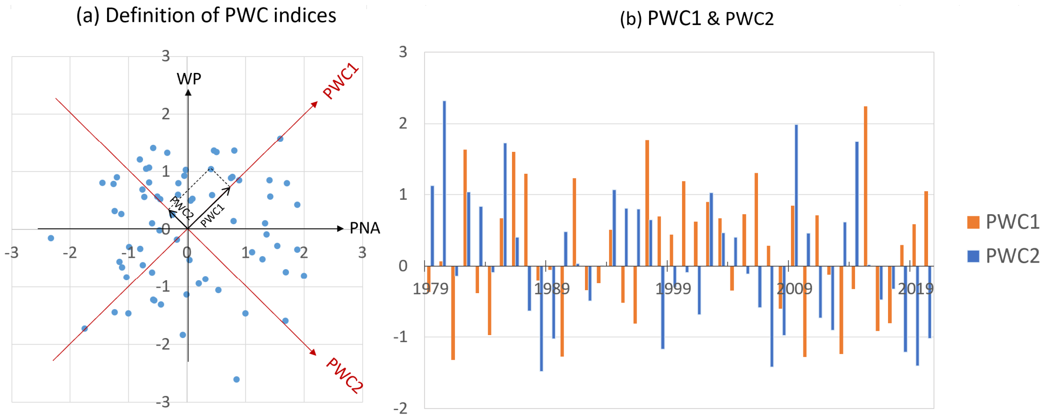

Figure 1 (a) The illustration of the definition of PNA and WP combined indices (PWC Index). (b) Time series of PWC1 and PWC2.

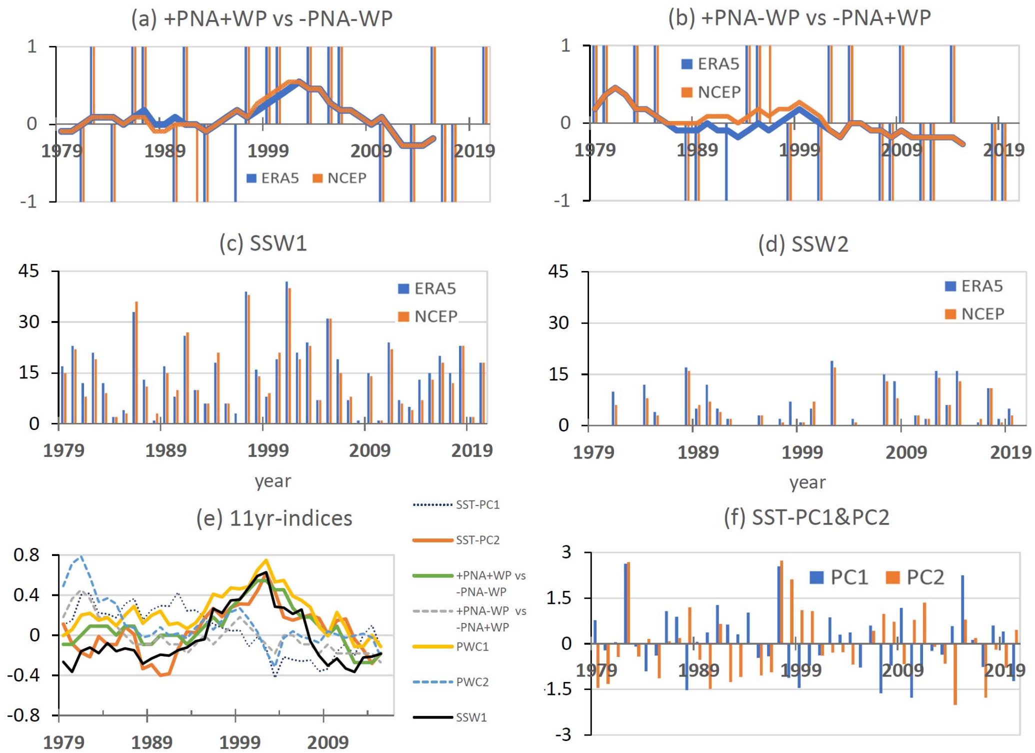

Figure 2 Time series from 1979 to 2020 of (a) +PNA+WP/−PNA−WP and (b) +PNA−WP/−PNA+WP. The duration (unit: day) of (c) SSW1 and (d) SSW2. (f) Two principal components of tropical Pacific SST. (e) 11-year moving averages of the climate indices from 1979 to 2015 (using the data from 1974 to 2020). The duration of SSW1 is normalized to compare with the moving averages of other indices.

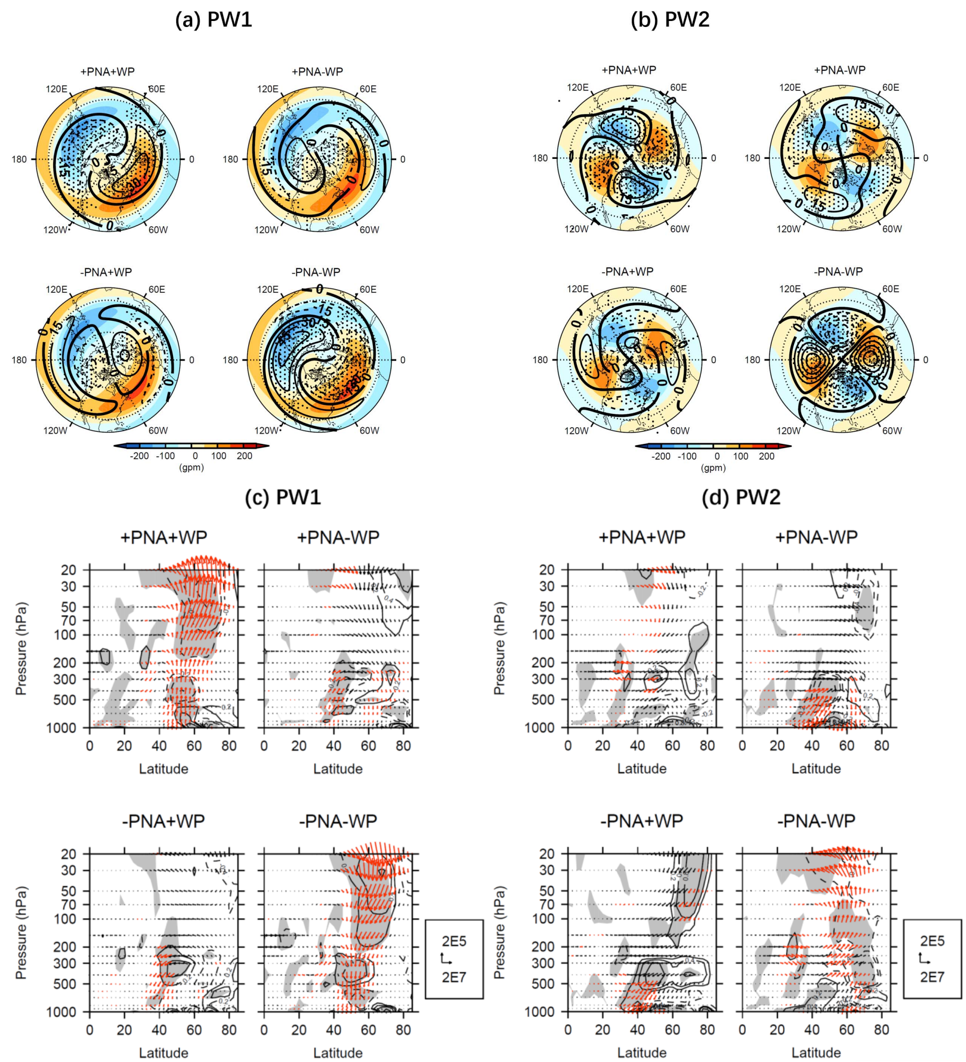

Figure 3 (a) PW1 and (b) PW2 components of the geopotential height anomalies at 200 hPa (black contour lines with the intervals of ±15, ±30, ±45 gpm; color-filled contours show the climatological mean) for different teleconnection combinations. PW1 (c) and PW2 (d) components of the EP flux (unit: m^3s^{-2}) and EP flux divergence (unit: $10^{-5}ms^{-2}$) anomalies. The regions of dots, red fluxes and grey divergence are significant at the 95% confidence level according to Student's *t*-test.

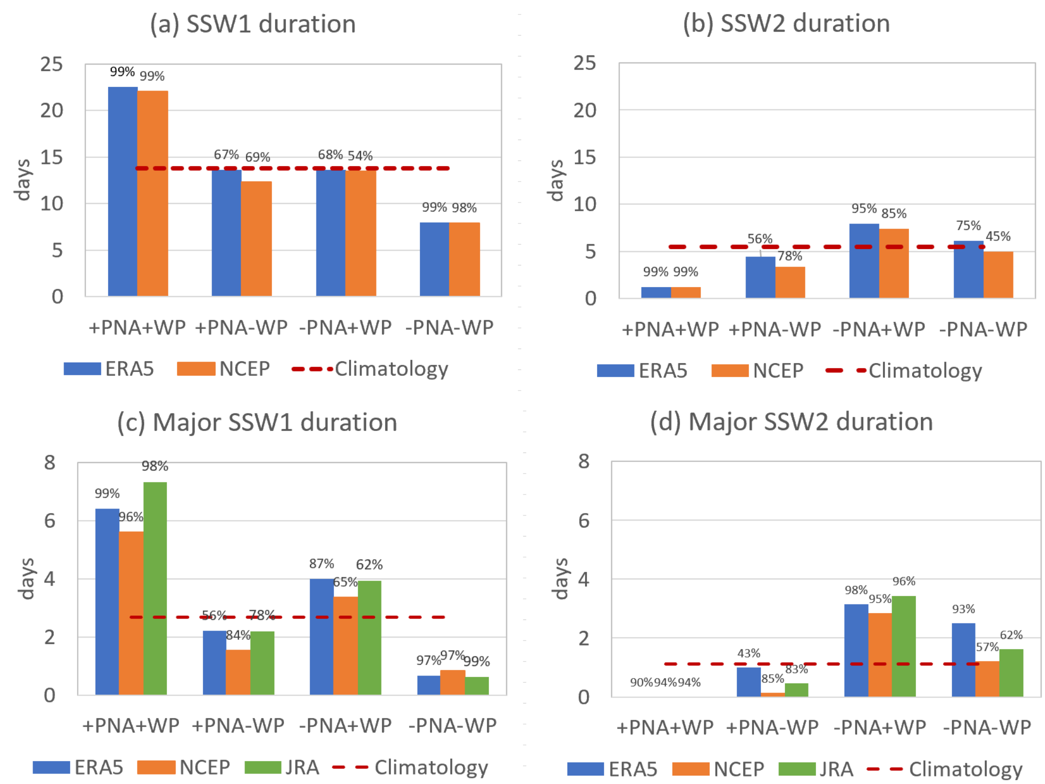

Figure 4 The duration of (a) SSW1, (b) SSW2, (c) major SSW1, and (d) major SSW2 corresponds to different combinations of the PNA and WP teleconnections. Monte Carlo test was used to calculate the statistical significance level of the deviations from climatology and the significance are labeled as percentage. Results of a and b are derived from ERA5 (1979-2020) and NCEP (1979-2020). Results of c and d are derived from ERA5(1950-2020), NCEP (1950-2020) and JRA55 (1958-2020).

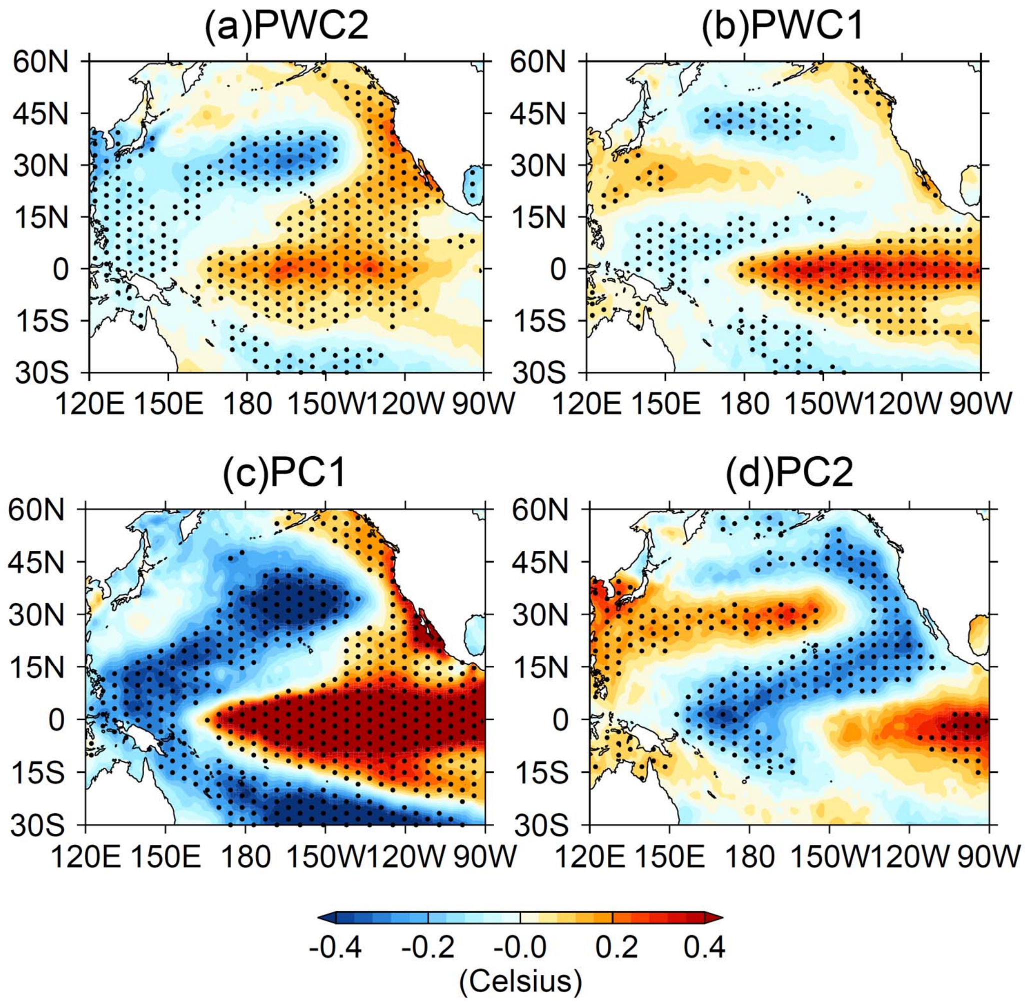

Figure 5 The SST anomalies regressed to (a,b) PWC Index and (c,d) tropical Pacific SST principal components. The regions of dots are significant at the 95% confidence level according to the F-test.

Figure 1.

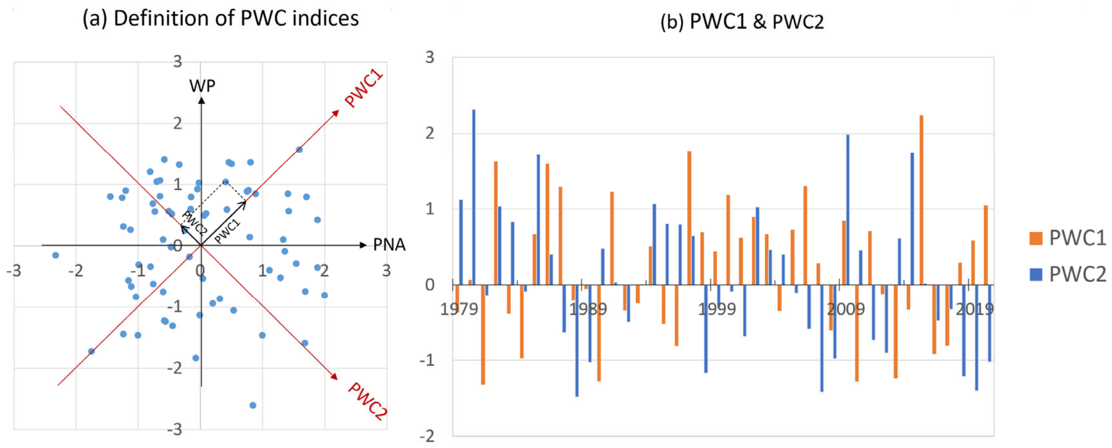

(a) Definition of PWC indices
WP
PNA
PWC1
PWC2
3
2
1
0
-1
-2
-3
(b) PWC1 & PWC2
1979
1989
1999
2009
2019
PWC1
PWC2

Figure 2.

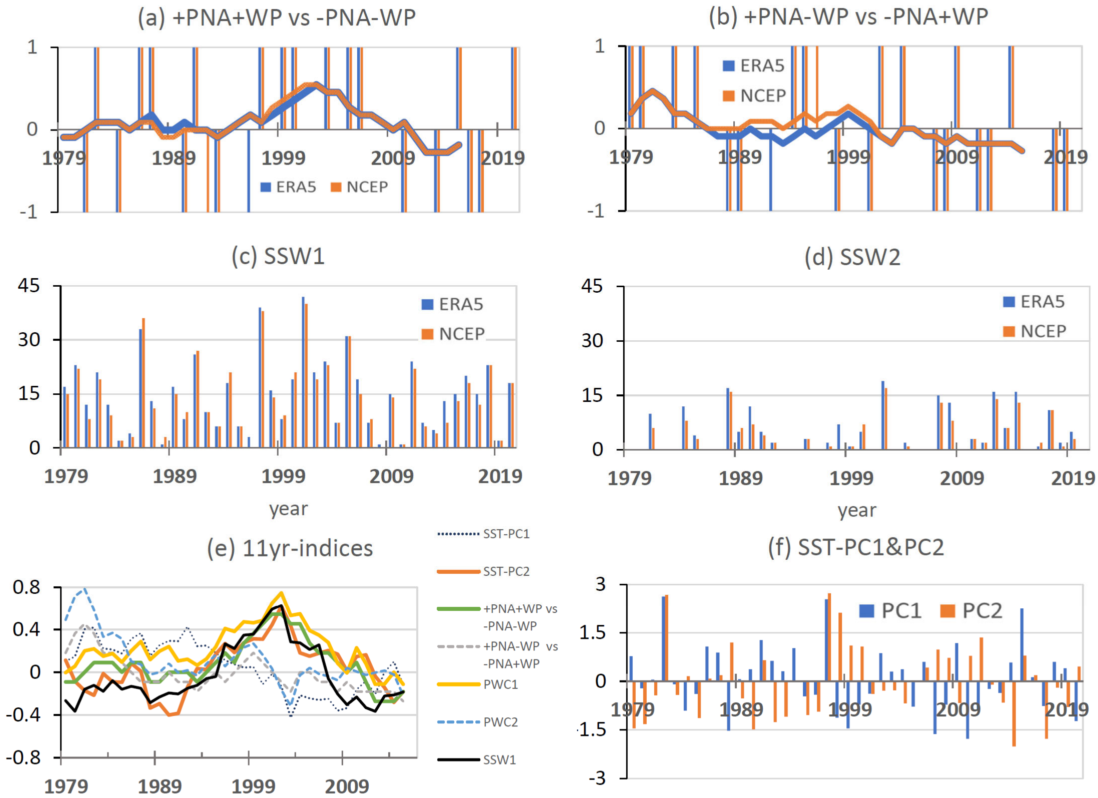

(a) +PNA+WP vs -PNA-WP
ERA5
NCEP
(b) +PNA-WP vs -PNA+WP
ERA5
NCEP
(c) SSW1
ERA5
NCEP
year
(d) SSW2
ERA5
NCEP
year
(e) 11yr-indices
SST-PC1
SST-PC2
+PNA+WP vs -PNA-WP
+PNA-WP vs -PNA+WP
PWC1
PWC2
SSW1
(f) SST-PC1&PC2
PC1
PC2

Figure 3.

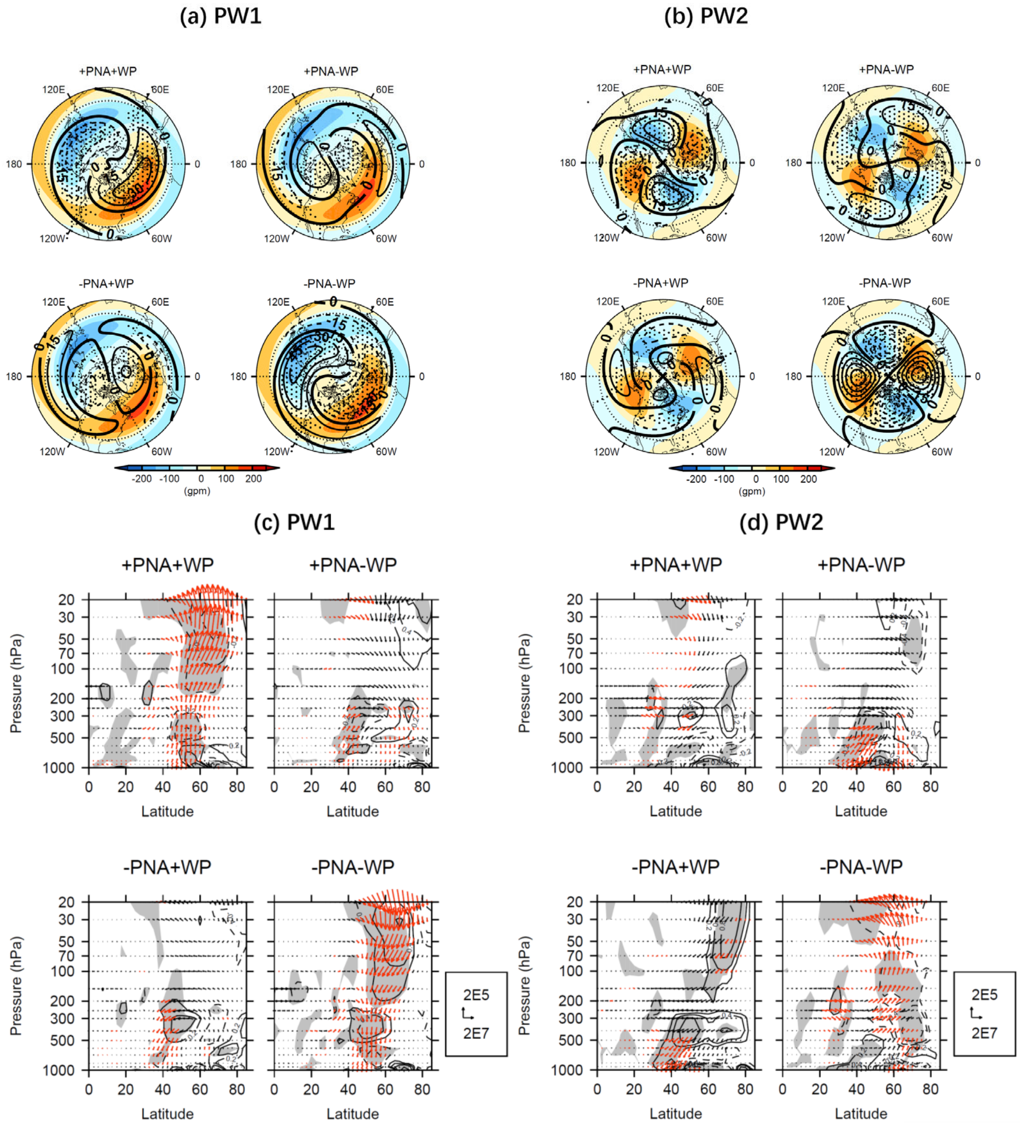
(a) PW1
(b) PW2
+PNA+WP
+PNA-WP
-PNA+WP
-PNA-WP
(gpm)
(c) PW1
(d) PW2
Pressure (hPa)
Latitude
2E5
2E7

Figure 4.

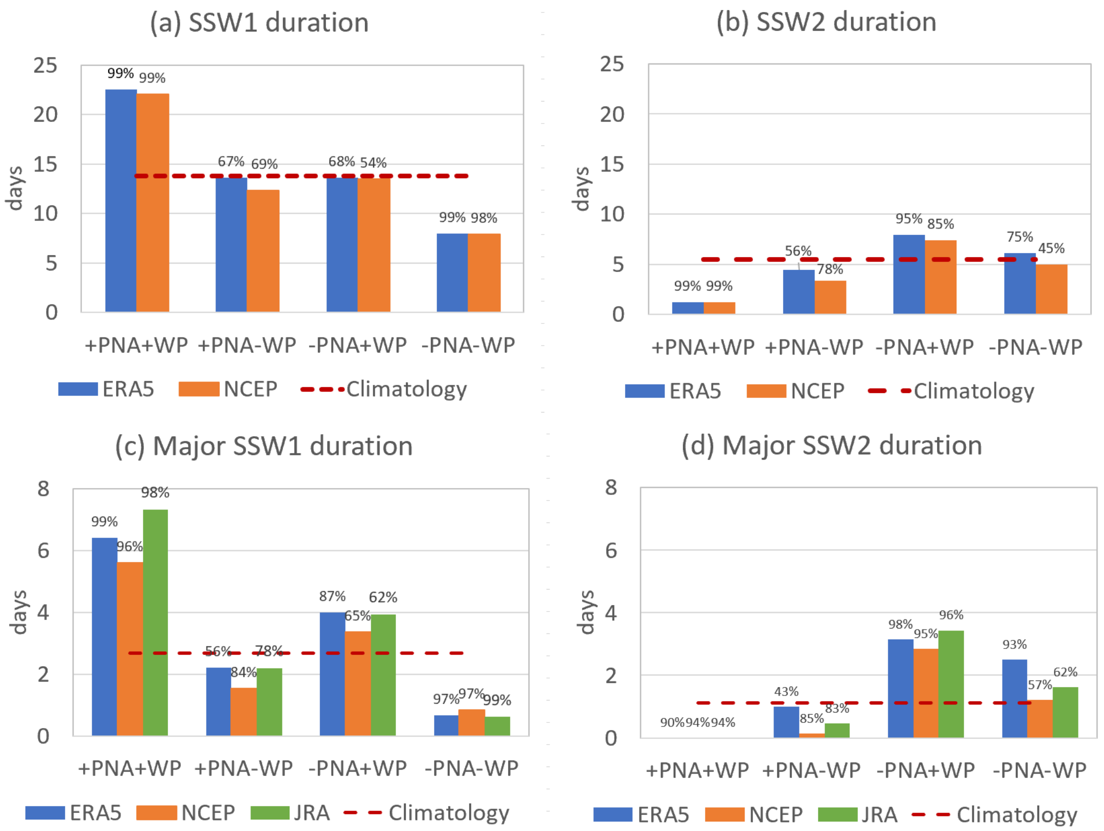

(a) SSW1 duration
days
25
20
15
10
5
0
99% 99%
67% 69%
68% 54%
99% 98%
+PNA+WP +PNA-WP -PNA+WP -PNA-WP
ERA5 NCEP Climatology
(b) SSW2 duration
days
25
20
15
10
5
0
99% 99%
56% 78%
95% 85%
75% 45%
+PNA+WP +PNA-WP -PNA+WP -PNA-WP
ERA5 NCEP Climatology
(c) Major SSW1 duration
days
8
6
4
2
0
99% 96% 98%
56% 84% 78%
87% 65% 62%
97% 97% 99%
+PNA+WP +PNA-WP -PNA+WP -PNA-WP
ERA5 NCEP JRA Climatology
(d) Major SSW2 duration
days
8
6
4
2
0
90% 94% 94%
43% 85% 83%
98% 95% 96%
93% 57% 62%
+PNA+WP +PNA-WP -PNA+WP -PNA-WP
ERA5 NCEP JRA Climatology

Figure 5.

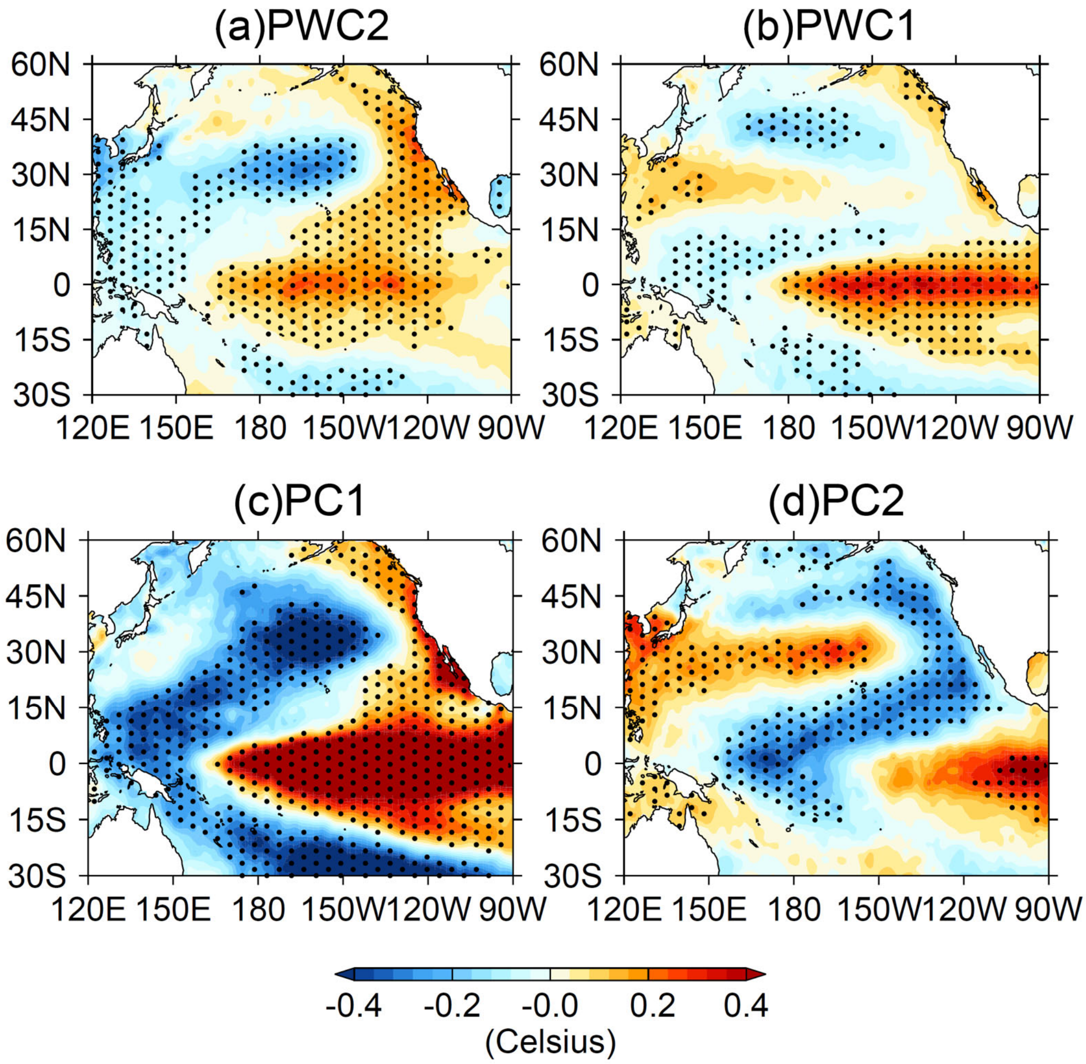

(a)PWC2
(b)PWC1
(c)PC1
(d)PC2
60N
45N
30N
15N
0
15S
30S
120E 150E 180 150W 120W 90W
-0.4 -0.2 -0.0 0.2 0.4
(Celsius)